Frequency Offset Estimation for Satellite Communications with Adaptive Frame Averaging

Julian Webber, Masanori Yofune, Kazuto Yano, Naoya Kukutsu, Kiyoshi Kobayashi and Tomoaki Kumagai
Advanced Telecommunications Research International, 2-2-2, Hikaridai, Seika-cho, Kyoto, 619-0288, Japan
{**jwebber, yofune_masanori, kzyano, kukutsu, kumagai**}**@atr.jp**

***Abstract*—The modified Luise and Reggiannini (L&R) algorithm is one of the frequency offset estimation algorithms suitable for use with the Digital Video Broadcasting - Satellite (DVB-S2) standard. Recently we demonstrated an enhanced poly-polarization multiplexing (EPPM) system incorporating L&R frequency recovery as a hardware prototype in order to evaluate its high spectral-efficiency in a real satellite channel. In order to provide sufficient performance at low SNR, it is recommended to average the correlation estimates over 2048 frames. In high SNR regions however, such a large averaging size is unnecessary. In this paper, two techniques are proposed in order to reduce the averaging size. The first technique measures the average noise power and selects an efficient frame averaging length using a noise look-up-table (LUT). The second technique uses a cyclic redundancy check (CRC) to determine if sufficient performance is achievable with the averaging size. Performance results show that the size of the averaging window can be reduced whilst maintaining a target BER. The noise LUT adaptive scheme has been implemented in hardware and we describe the real-time behavior.**

***Keywords*—**satellite communications, polarization multiplexing, frequency offset estimation, latency reduction, performance investigation, hardware implementation.

I. Introduction

High spectral efficiency is especially important in satellite communications due to the constraints of limited transmit power and fixed-bandwidth whilst facing ever-increasing demands on data throughput. The recent DVB-S2X standards extension [1] has brought a number of new design features that increase the spectral efficiency. Increasing the modulation order on each polarization is a common technique to increase the throughput. Although multiple-input multiple-output (MIMO) techniques have revolutionized the mobile communications space, it is less straight-forward to apply them to satellite systems due to the very strong line-of-site channel. In this work, the base-system uses a concept of multiple polarizations, and we focus on the system frequency recovery.

Most modern transponders operate a scheme called orthogonal polarization multiplexing (OPM) in which they simultaneously transmit on vertical (V) and horizontal (H), or lefthand and righthand circular, polarizations and achieve sufficient isolation. Multiplexing more than two signals onto the V and H channels creates interference that cannot be removed by a linear spatial filter as the number of independent paths is limited to two. However, by appropriately selecting the signal constellations at the transmitter and applying powerful digital signal processing techniques at the receiver, it is possible to recover the signals and achieve significant efficiency gains compared to the conventional OPM system.

In general, stricter requirements are made on the phase and frequency recovery algorithms as the modulation order increases. Improved frequency and phase accuracy are therefore becoming important issues with extensions to 256-APSK modulation listed in DVB-S2X and also in our multi-polarization system. Estimation performance can be improved by increasing the UW length and increasing the frame averaging size used in the phase estimation. Here we investigate an adaptive architecture that reduces the frame averaging size while aiming to maintain error performances.

There have been a number of research proposals relating to the optimization of correlation based frequency recovery algorithms. A technique to optimize the correlation length depending on the frequency offset was proposed for the L&R in [2]. In this paper we aim to optimize the frame averaging size, L. We first proposed the adaptive-L by noise estimation (herein termed ALNE) architecture in [3] and we extend that work to describe the hardware performance. In addition, we propose an alternative technique called adaptive-L by CRC (ALC).

This paper is organized as follows. The EPPM technique is briefly introduced in Section II. The frequency estimation and correction method is described in Section III. The ALNE and ALC architectures are detailed in Section IV and V respectively. A software performance investigation is presented

Manuscript received Oct 31, 2014. This work is supported by Japan Ministry of Internal Affairs and Communications with the fund of "Research and Development of Capacity Enhancing Technology for Satellite Communications by Employing Dynamic Polarization and Frequency Control.

J. Webber is with the Wave Engineering Laboratory, Advanced Telecommunications Research Institute International (ATR), Kyoto, 619-0288, Japan. (Tel: +81-774951313; email: jwebber@atr.jp).

M. Yofune is with the Wave Engineering Laboratory, Advanced Telecommunications Research Institute International (ATR), Kyoto, 619-0288, Japan. (email: yofune_masanori@atr.jp).

K. Yano is with the Wave Engineering Laboratory, Advanced Telecommunications Research Institute International (ATR), Kyoto, 619-0288, Japan. (email: kzyano@atr.jp).

N. Kukutsu is with the Wave Engineering Laboratory, Advanced Telecommunications Research Institute International (ATR), Kyoto, 619-0288, Japan. (email: kukutsu@atr.jp).

K. Kobayashi was with the Wave Engineering Laboratory, Advanced Telecommunications Research Institute International (ATR), Kyoto, 619-0288, Japan. He is now with NTT Access Network Service Systems Laboratories, 1-1, Hikarinooka, Yokosuka, Japan. (email: kobayashi.kiyoshi@lab.ntt.co.jp).

T. Kumagai is with the Wave Engineering Laboratory, Advanced Telecommunications Research Institute International (ATR), Kyoto, 619-0288, Japan. (email: kumagai@atr.jp).

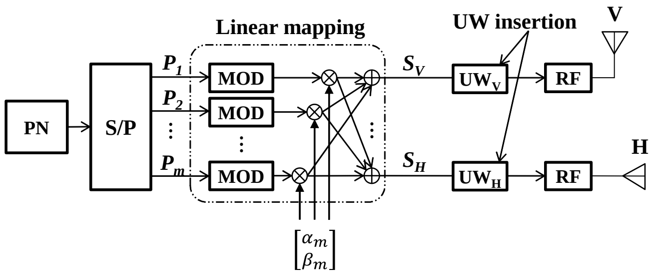

Fig. 1. EPPM transmitter architecture.

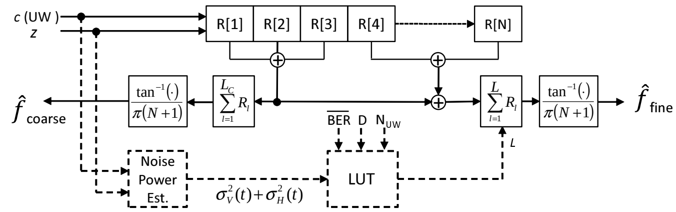

Fig. 2. Block diagram of the frequency recovery showing the additional architecture for noise power estimation with LUT for L.

in Section VI and a discussion of the hardware design in Section VII. Finally a conclusion is drawn in Section VIII.

II. Enhanced Poly-Polarization Multiplexing

The enhanced poly-polarization multiplexing (EPPM) system transmitter architecture is shown in Fig. 1. In the EPPM system, the H and V components of the n-th transmitted symbol, $T_H(n)$, $T_V(n)$ are expressed as

$$\left[\begin{array}{c} T_H(n) \\ T_V(n) \end{array}\right] = \sum_{m=1}^{M} \left(\left[\begin{array}{c} \alpha_m \\ \beta_m \end{array}\right] X_m(n) \right) \tag{1}$$

where $X_m(n)$ is the m-th stream transmit data symbol to be modulated, α_m, β_m are generalized complex mapping coefficients. An optimized set of mapping coefficients are computed offline by searching for a constellation set that has the maximum minimum-Euclidean distance. The enhanced PPM scheme is a superset that includes the basic PPM scheme. In PPM, a polarization angle between the V and H planes determines the I-Q constellation points on the additional polarization planes. In the simulations in this paper, we transmit on 3 data streams, corresponding to a polarization angle of 45 degrees, with QPSK modulation on each stream. Further details of the technique are described in [4].

III. Frequency offset estimation

In order to estimate the frequency offset and channel state information (CSI), an orthogonal Gold code unique word (UW) is inserted at the start of each frame on V and H polarizations. The UW length is between 64 and 256 symbols is inserted and should be minimized in order to maximize the effective bandwidth efficiency. The target in this paper is to reduce the length from N_{UW}=256 to 64 symbols while maintaining the performance.

The L&R frequency offset [5], $\hat{f}_{LR}$ is estimated from the argument of the sum of correlations, R. The so-called 'modified L&R' computes an average correlation over L preceding frames prior to calculating the argument and improves the performance in noise [6].

$$\hat{f}_{LR} = \frac{1}{\pi T_s(N+1)} \arg \sum_{l=B-L+1}^{B} \sum_{k=1}^{N/2} \frac{1}{N-k} R(k,l) \tag{2}$$

$$R(k,l) = \sum_{i=k+1}^{N} x(i,l)x^*(i-k,l) \tag{3}$$

where T_s is the symbol period, B is the current frame number, $x(i,l)$ is the UW pilot at position i of frame l, and N is the correlation length, N_{UW}/2 in this paper.

The frequency recovery consists of four estimators: a coarse feedback loop and fine feed-forward loop on each of the V and H channels. The architecture of a single-branch is shown by the continuous lines in Fig. 2. The optimum performance of the fine recovery loop is achieved by setting the correlation length equal to half the UW size, as it achieves the Cramer-Rao lower-bound on the estimation error [5]. The coarse loop has a reduced length of between 2-6 symbol delays in order to achieve a large frequency pull-in range.

A. Frame Averaging

The potential benefits of frame averaging were investigated by calculating the average residual frequency offset as a function of the correlation length, N and averaging length, L. The performance of a N_{UW}=256 system, at E_b/N_0=14 dB, symbol-rate 1.6 MBaud and assuming a ± 3.2 kHz frequency offset on V and H is shown in Fig. 3. It can be seen that the absolute residual offset can be substantially reduced by frame averaging. The residual error reduces at about the same rate with L for a given value of N. The graph shows that it is possible to trade-off L and N in order to achieve a required maximum residual offset. In this work however, we restrict the value of N to half the UW length, in order to simplify an adaptive implementation in hardware. Although the cost of programmable logic memory is now relatively low, it is beneficial to limit excessive values of L particularly in conditions where the offset has high temporal variation. This situation can arise when the phase noise is high or there is movement of, or within the vicinity of, the satellite user-station causing Doppler shift. In a practical system, an average tolerable frequency offset is determined based on the particular quality of service (QoS) requirements. In the next section we propose a method to select L adaptively.

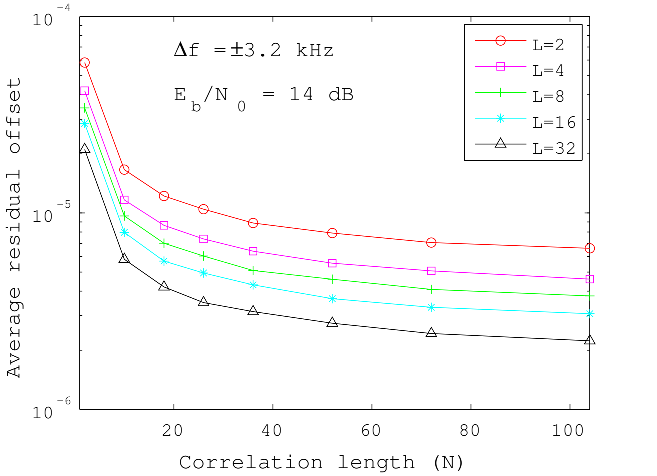

Fig. 3. Average normalized residual frequency offset versus correlation length for different averaging lengths L.

B. Distributed Unique Word structure

In general, frequency estimation performance degrades when shorter UW lengths are used as there are less symbols used and the maximum distance between them is less. We have recently shown that the estimation performance can be improved by increasing the distance between the UW constituent symbols for a given UW length [7]. This technique improves the estimation performance at low values of L and enables the benefits of the adaptive architectures to be further exploited by short UW lengths. The distribution of UW symbols on V-polarization with a constant separation of D=4 are shown in Fig. 4. The data symbols are sandwiched between the UW symbols and the remainder are placed together after the last UW symbol. In the receiver, the distributed UW symbols are repacked into a continuous memory array of length N_{UW}. The frequency estimate is then obtained by dividing the standard L&R estimate with the spacing, D. The variable D is a system-level parameter that needs to be known at both the transmitter and receiver. Therefore it is set at the start-of-packet and remains constant for the entire transmission.

IV. Adaptive-L by Noise Estimation (ALNE)

The frame averaging length is selected based on the average estimated noise power jointly measured on the V and H channels. The basic modified L&R algorithm forms the architecture basis. The additional components comprise a noise estimation process and a look-up table (LUT) containing appropriate averaging lengths. The modifications are indicated by the dashed lines in Fig. 2.

The normalized noise power on each branch, $\sigma^2_{V/H}$ is estimated by subtracting the known transmitted signal component from that of the received signal plus noise. An average value is calculated across N pilots and a sliding-window of W frames

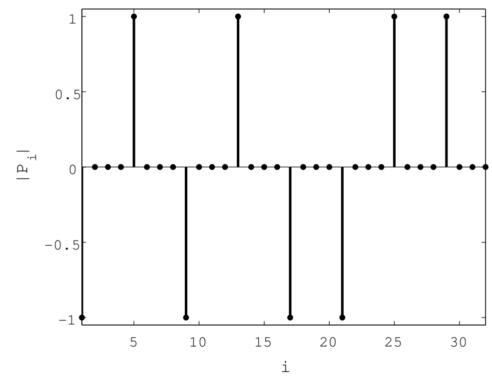

Fig. 4. The first 8 UW symbols with a constant spacing of D=4 separated by data symbols.

TABLE I. ALNE Look-up-table contents.

Index	Lower bound	Upper bound	L
0	0.18	1.00	4096
1	0.12	0.18	1024
2	0.06	0.12	512
3	0.04	0.06	256
4	0.028	0.04	128
5	0.02	0.028	64
6	0.012	0.02	16
7	0.00	0.012	4

as

$$\sigma^2_V(t) = \frac{1}{WN}\sum_{n=t-W}^{t}\sum_{m=1}^{N}|r_V(n,m)|^2 - |r_V(n,m)x^*_V(m)|^2 \quad (4)$$

$$\sigma^2_H(t) = \frac{1}{WN}\sum_{n=t-W}^{t}\sum_{m=1}^{N}|r_H(n,m)|^2 - |r_H(n,m)x^*_H(m)|^2 \quad (5)$$

where, x_V and x_H are the transmitted UW on V and H polarizations, r_V and r_H are the received UW signals on V and H polarizations. An average of the two branches is computed as

$$\sigma^2_{VH}(t) = \frac{1}{2}(\sigma^2_V(t) + \sigma^2_H(t)) \quad (6)$$

The average noise power indexes a LUT containing values of L. The default LUT contains eight entries for the noise boundaries and the associated values for L, as listed in Table I and plotted in Fig. 5. The size of L is a power of two, to make efficient use of reserved memory. Noise boundaries should be pre-computed off-line through a study of BER performance simulations with different L. The LUT can be expanded if more optimal values are determined and can be updated at run-time via a GUI interface.

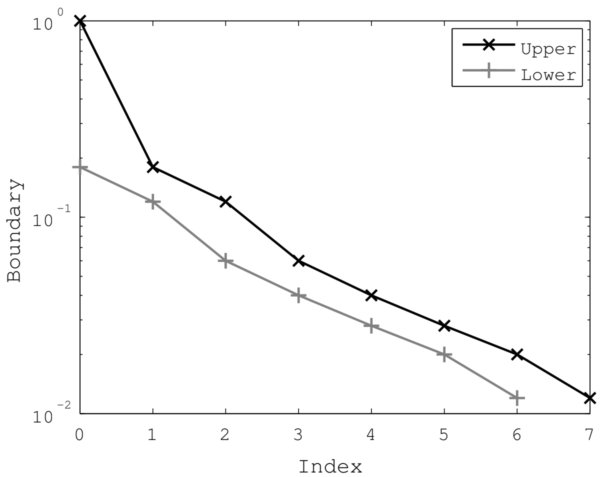

Fig. 5. Plot of the ALNE look-up-table boundaries.

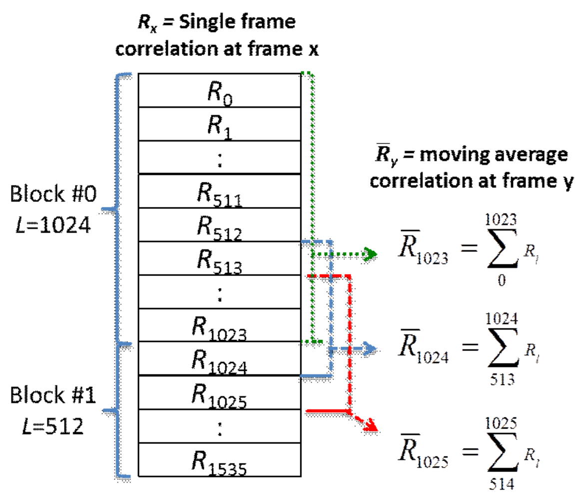

Fig. 6. Calculating the moving average correlation $\bar{R}$ with example of updating the value of L at frame 1024.

At start-up, the memory containing the correlation values is empty and hence the procedure to update L is delayed until the memory buffer is sufficiently full. An example showing the memory structure for the first 1536 frames and associated correlation computations is shown in Fig. 6. The correlation average, $\bar{R}_{1023}$, is computed from frames 0 to 1023 inclusive. After determining the new value of L to be 512, the window is updated to cover frames 513 to 1024. The correlations computed at frames 514 to 1025 are used to calculate the average correlation for frame 1025, and so on.

V. Adaptive-L by CRC (ALC)

In this second architecture, the Tx appends a cyclic redundancy check (CRC) symbol to the end of each frame as shown in Fig. 7. A value of D is set at both the Tx and Rx and is held constant throughout the transmission. At the Rx,

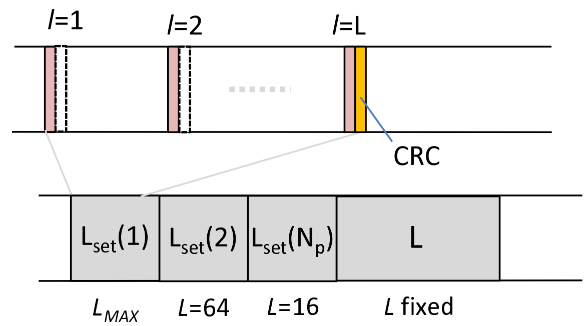

Fig. 7. ALC packet structure showing (top) CRC symbol appended after L frames (bottom) N_L blocks with decreasing value of L followed by transmission with fixed L

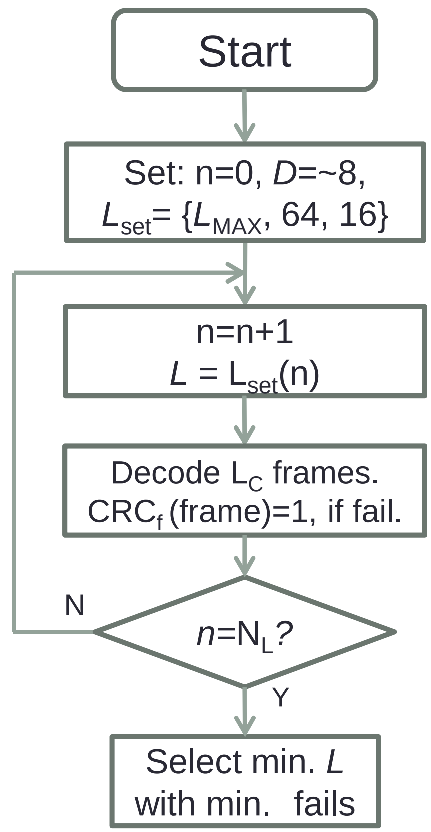

Fig. 8. ALC flowchart for determining the value of L.

a set of L descending values is specified before the start of packet reception, e.g. $L_{set} = \{L_{MAX}, 64, 16\}$, where L_{MAX}, is the maximum value of L to be tested (Fig. 8). It can be set according to the satellite frequency band, D, or MCS. If the channel has a low SNR or a high modulation scheme is used, L_{MAX} is set high e.g. 768. If the channel has high SNR or a high value of D is set, L_{MAX} can be reduced e.g. 128.

After L_{MAX} frames have been received, a frequency estimate is made by averaging the L correlation values.

TABLE II. SIMULATION PROPERTIES.

UW code	Orthogonal Gold
UW length (N_{UW})	64, 256
Data length	2304 symbols / stream
Modulation	3-streams @ QPSK
Freq. offset	±2,4 kHz
Frequency recovery	Modified L&R
Baud rate	1.6M, 3.2M
FEC	None, LDPC (R=5/6)
Channel	AWGN

The l-th frame data is then demodulated and $Rx_{CRC}(l)$ obtained. $Tx_{CRC}(l)$ is then compared with $Rx_{CRC}(l)$. If $Rx_{CRC}(l) \neq Tx_{CRC}(l)$, a CRC fail variable Fail(n) is incremented. Next, $Tx_{CRC}(l$+1) is compared with $Rx_{CRC}(l$+1). Then n is incremented to 1 and the Rx next sets L=$L_{set}(1)$. As $L_{set}(1) < L_{set}(0)$ the averaging process, and hence frequency offset estimation, can actually be done using the correlation contents already held in memory and thus without any wasteful retransmissions. The smallest value of L that passes the CRC test is finally selected.

VI. Software Simulation

A performance evaluation was conducted for the EPPM system using the parameters shown in Table II. Random PN data of length 2 bits × 2304 symbols was generated for each of three streams. The stream data was mapped onto the two polarizations using EPPM modulation and a UW preamble inserted of length N_{UW}. The data packet was convolved with a root raised cosine filter having roll-off factor α=0.5. A ± 4 kHz frequency offset was applied to V & H. At the receiver, AWGN is added and the signal matched filtered and down-sampled. The UW sections are extracted and the frequency offsets corrected on both V and H-channels. The noise level is averaged over 32 symbols and indexes the LUT. The data was estimated by MLD processing. The BER measurements started after 2048 frames (i.e. the correlation memory was full for all values of L) and the first value of L had been selected from the LUT.

The BER performance for N_{UW}=64 is plotted in Fig. 9 and shows that when the UW length is short and the UW symbols are adjacent to each other (D=1), the performance is degraded by selecting small values of L. As E_b/N_0 increases however, L can be reduced whilst maintaining a given BER. By increasing the UW symbol spacing to D=8, the performances for low-values of L are substantially improved as shown in Fig. 10. At the BER 1E-4, it can be seen that L can be reduced from 2048 to 128, with a negligeable loss in performance. The BER performance for N_{UW}=256 is plotted in Fig. 11. It can be seen that L can be set to 128 with little performance loss compared to the maximum value.

The required value of E_b/N_0 to achieve an error rate of 1E-4, as L increases for a fixed value of D, is plotted in Fig. 12. A plateau shows the region where there is little additional benefit from increasing the value of L further. It can be seen that

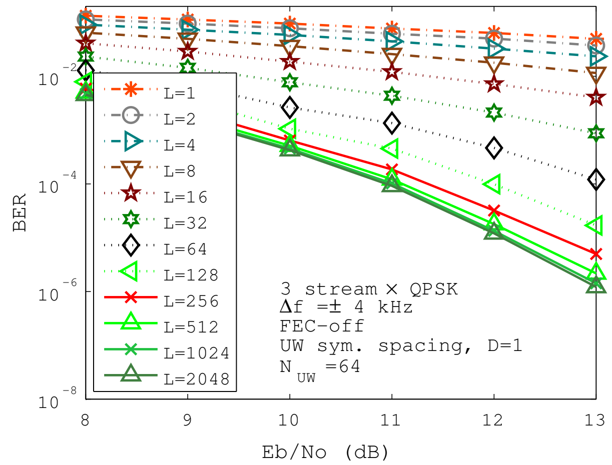

Fig. 9. BER performance of 3 stream × QPSK, N_{UW}=64 with UW symbol spacing D=1.

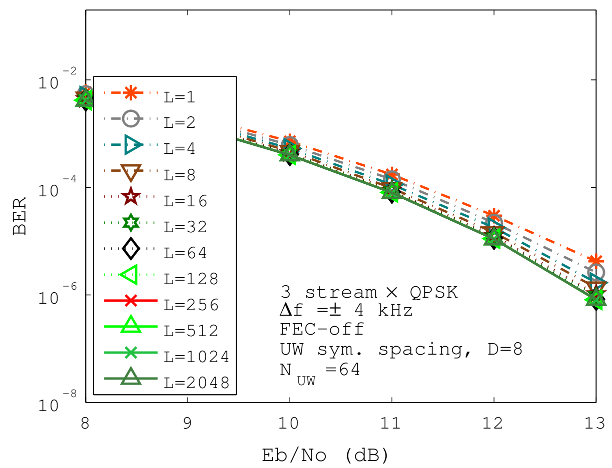

Fig. 10. BER performance of 3 stream × QPSK, N_{UW}=64 with UW symbol spacing D=8.

L=512 is an efficient setting for the case $\{N_{UW}$=64, D=2$\}$. In the case of $\{N_{UW}$=256, D=1$\}$ and $\{N_{UW}$=64, D=4,8$\}$, L can be set to 64 without any observable degradation in performance.

The reduction in the size of L compared to a fixed value of 1024 is shown in Fig. 13 for the case of N_{UW}=64. With symbol spacing D=2, the averaging length can be reduced by about 75% whilst maintaining the target BER at 1E-4. In the case of LDPC with D=4, L can be optimally set to 512 at 4.8 dB and decreased to 32 at 6.0 dB. The optimized settings depend on the particular modulation coding scheme (MCS) and a specific LUT for each MCS should be investigated as part of our future work.

A BER simulation was set-up to investigate the ALC behavior. Three simulations with a different value of D=$\{8,16,32\}$ were conducted. At the transmitter, EPPM 6-bit modulation

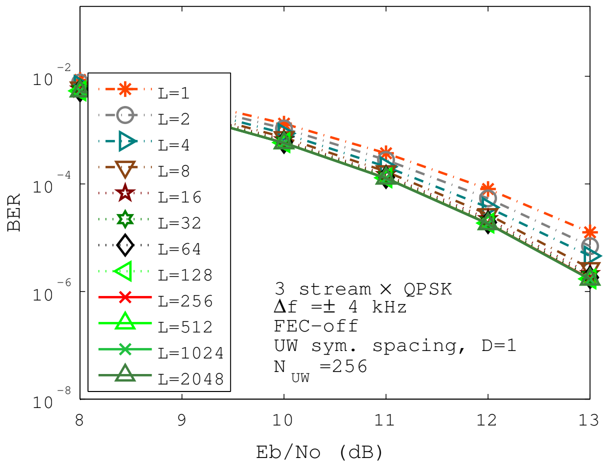

Fig. 11. BER performance of 3 stream × QPSK, N_{UW}=256 with UW symbol spacing D=1.

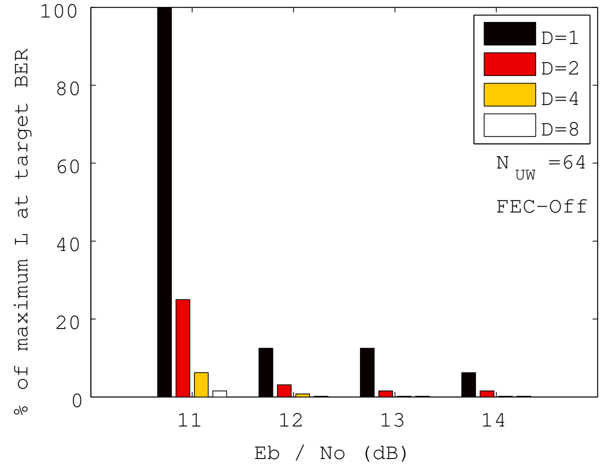

Fig. 13. Percentage in size of L relative to fixing L=1024 whilst maintaining a target BER of 1E-4 for N_{UW}=64 without LDPC.

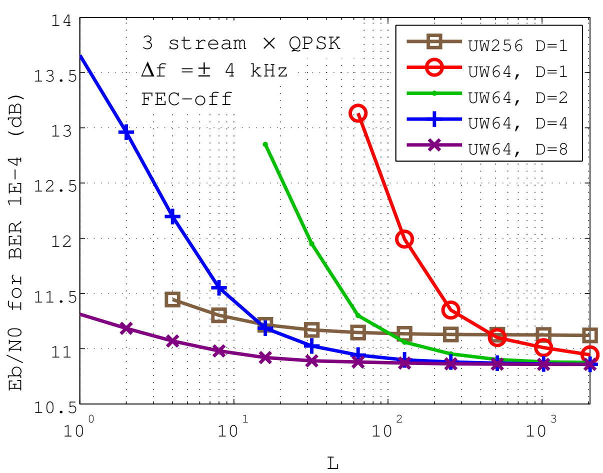

Fig. 12. Required E_b/N_0 to achieve an uncoded BER of 1E-4 as L increases.

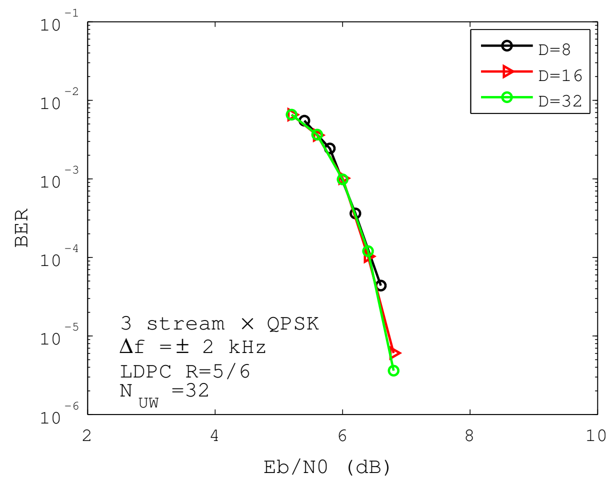

Fig. 14. ALC error performance for D={8,16,32} with ± 2 kHz offset.

with coding rate was R=5/6 was applied. At the receiver, a ± 2 kHz offset was added. The frame averaging size was determined by the adaptive algorithm which selects a value of L that achieves the desired lowest sum of CRC fails. Without, the ALC control, the significantly different D for a fixed value of L would result in different BER. However, the error graph shows that each transmission had almost identical performance (Fig. 14). When a low value of D was used, a larger value of L was selected automatically in compensation.

Both ALC and ALNE use different techniques to achieve the same aim. In terms of complexity, the ALNE is preferred as the noise estimation requires relatively few hardware multiplications and has no CRC overhead. Further, the noise estimation may already be required and computed by the LDPC block. The ALC could however be considered if a CRC module is already part of the system design.

VII. Hardware Implementation

Each transceiver board consists of five Xilinx FPGAs with the frequency recovery and signal processing operations computed on a Virtex XC6SLX100 device. The symbol rate is variable between 0.05-10 MBaud, the input sampling rate is 102.4 MHz. The ADC and DAC precisions were 12-bits and 16-bits respectively. The transmitter and receiver settings are entered via a GUI on the respective Tx and Rx PCs. The required E_b/N_0, frequency and phase offsets were set on a SLE900 satellite channel emulator. The transceiver system is shown in Fig. 15 and further details of the design are in [8]. The BER is computed by comparing the transmitted and received signals using an Anritsu MP8931A BER tester.

The estimated frequency offset on each polarization as measured in hardware is plotted in Fig. 16. The value of D=12 and L was determined by LUT. The estimated offset

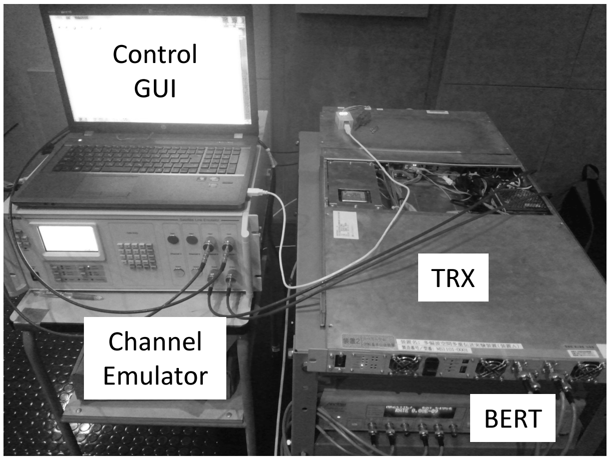

Fig. 15. Satellite testbed system comprising Tx, channel emulator, Rx and BER tester.

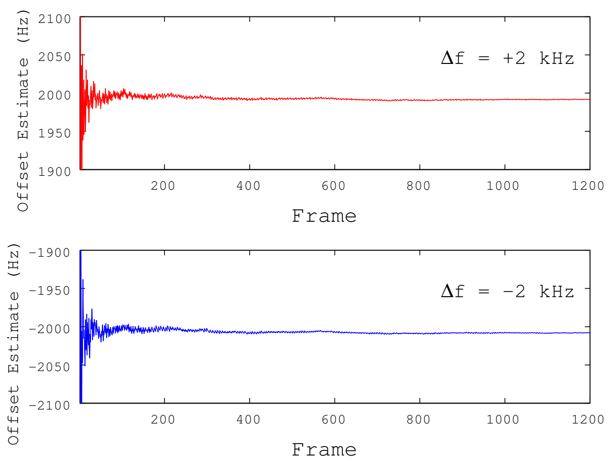

Fig. 16. Frequency offset estimate in hardware in response to a $\pm$ 2 kHz offset set by the channel emulator (top) H-polarization, (bottom) V-polarization.

was within $\pm$ 8 Hz of the value set in the channel emulator with 10 dB SNR.

A. Adaptive-L by Noise Estimation

The LUT in hardware was verified by examining frame versus index results data. The SNR on the SLE channel emulator was varied from 10 dB to 20 dB in steps of 2 dB. The frame number at which the index changed is written to file and from this the variation of L with frame number is plotted in Fig. 17. After switching on the machine, the LUT is filled with correlation data. At position O an SNR of 10 dB is set with the addition switch off in the channel emulator and hence L reverts to the low value of 16. At position A_1, noise addition is switched on and quickly the value of L changes to 1024 at postion A_2. It stays at this position for about 6000 frames. It briefly reduces to 512 but then returns to 1024. At position A_3, the noise is switched off and the value of L rapidly

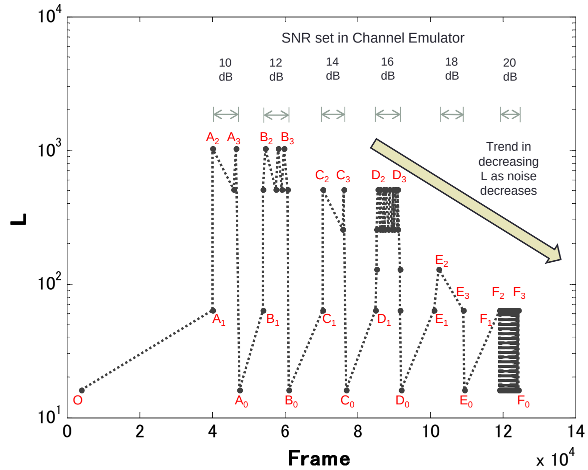

Fig. 17. Variation of L versus frame as SNR increases from ALNE hardware experiment.

reduces to 16. A similar process is repeated for the remaining SNR values. That is, the SNR is set to $\{12,14,16,18,20\}$ dB at positions $\{B_1,C_1,D_1,E_1,F_1\}$ respectively. The respective noise is added until positions $\{B_3,C_3,D_3,E_3,F_3\}$ respectively.

Two further general observations can be made from this figure. First, there is a downward trend in L observed as the SNR increases and confirms the desired behavior. The exact SNR at which the value of L changes depends on the LUT boundary entries and whose determination is an off-line optimization task to achieve a desired performance. Second, occasionaly (e.g. D_2 to D_3) there are oscillations between two values of L. When L is large, the estimation performance is high and the estimation is very accurate. A lower value of L is subsequently selected by the algorithm. The estimation performance degrades slightly and subsequently a higher value of L is required. To avoid the averaging size being updated too frequently, control circuitry should manage the case when the measured noise power oscillates across a LUT boundary. This situation becomes more important when the LUT is small and thus there are relatively large steps of L.

Various techniques can be applied to control the oscillatory behavior. A hysteresis can be set so that the new setting of L only becomes valid if the boundary is crossed for a sufficient number of frames. Alternatively, the update rate for L can be set to once per a given number of frames. The optimization can also achieved by adjusting the boundary positions or changing the frame averaging LUT entries. This optimization together with the hysteresis should be added as a future upgrade to the firmware. A software simulation with $\{D$=12, L=256$\}$ was compared with hardware results for D=12 with L determined by LUT. There is a close match between the software and hardware performances as shown in Fig. 18. LUT-B achieves slightly better performance than LUT-A due to a larger value of L being used.

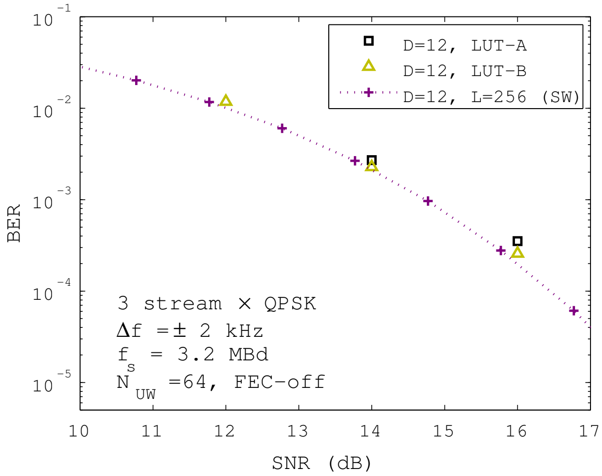

Fig. 18. BER of ALNE in hardware for uncoded 6-bit EPPM with ± 2 kHz offset, 3.2 MBaud, D=12.

VIII. Conclusion

We have proposed two adaptive techniques to reduce the frame averaging required in satellite frequency offset estimation. These techniques are called adaptive-L by noise estimation (ALNE) and adaptive-L by CRC (ALC). In ALNE, the window-size for frame averaging was reduced by selecting it based on the estimated noise power on both V and H branches. A BER of 1E-4 could be maintained with a reduction in L of 75% for D=2 with UW length 64 at 11 dB E_b/N_0. The particular algorithm selection partly depends on implementation complexity and whether CRC and noise estimation modules are already used in other parts of the system. Further work should optimize the performance by adding a hysteresis to avoid excessive switching between boundaries and optimize the averaging sizes for the LUT across a range of MCS and channel conditions.

Acknowledgment

This work is supported by Japan Ministry of Internal Affairs and Communications with the fund of "Research and Development of Capacity Enhancing Technology for Satellite Communications by Employing Dynamic Polarization and Frequency Control."

References

[1] DVB Project Office, "DVB-S2X - S2 extensions: Second generation satellite extensions," *DVB Fact Sheet*, May. 2014.

[2] F. Gong, G. Shang and K. Peng, "Initial estimation based adaptive carrier recovery scheme for DVB-S2 system," *IEEE Transactions on Broadcasting*, Vol. 58, No. 4, Dec. 2012.

[3] J. Webber, M. Yofune, K. Yano, H. Ban, K. Kukutsu and K. Kobayashi, "Adaptive frequency offset estimation for practical satellite communication channels," *IEEE International Conference on Advanced Communications Technology*, Korea, 16-19th Feb. 2014.

[4] M. Yofune, J. Webber, K. Yano, H. Ban, and K. Kobayashi, "Optimization of signal design for poly-polarization multiplexing in satellite communications," *IEEE Commun. Letters*, pp. 2017–2020, vol. 17, no. 11, 2013.

[5] M. Luise and R. Reggiannini, "Carrier frequency recovery in all-digital modems for burst-mode transmissions," *IEEE Trans. Commun.*, vol. 43, no. 2/3/4, pp. 1169–1178, Feb-Apr. 1995.

[6] ETSI "Digital Video Broadcasting (DVB) User guidelines for the second generation system for broadcasting, interactive services, news gathering and other broadband satellite applications (DVB-S2)," *ETSI Technical Document TR 102 376 v1.1.1*, Sophia Antipolis, Feb. 2005.

[7] J. Webber, M. Yofune, K. Yano, H. Ban, and K. Kobayashi, "Performance of frequency recovery algorithms for a poly-polarization multiplexing satellite system," *IEEE Malaysia International Conference on Communications (MICC'13)*, Malaysia, Nov. 2013.

[8] J. Webber, M. Yofune, K. Yano, H. Ban, and K. Kobayashi, "Experimental evaluation of a poly-polarization multiplexing system with timing/frequency recovery for satellite communications," *AIAA International Communications Satellite Systems Conference (ICSSC'13)*, Florence, Italy, Oct. 2013.

Julian WEBBER received the M.Eng. and Ph.D. degrees from the University of Bristol, UK in 1996 and 2004 respectively. From 1996-98, he was with Texas Instruments, Europe engaged on ASIC and DSP systems. From 2001-07 he was employed as a Research Fellow at Bristol University engaged in real-time MIMO-OFDM testbed implementation, and from 2007-12 he was a Research Fellow at Hokkaido University, Sapporo, Japan, working on MIMO signal processing & wireless communications. He is currently a researcher at ATR, Kyoto, Japan principally working on frequency recovery and spectrally efficient modulation techniques for satellite communications. His other current research interests include MIMO, high resolution direction of arrival estimation and M2M. He is a member of the IEEE and IEICE.

Masanori Yofune received the B.E. and M.S. degrees in systems engineering from Hiroshima City University, Hiroshima, Japan, in 2008 and 2010, respectively. In 2010, he joined Mobile Techno Corporation, Kawasaki, Japan, where he has been engaged in research and development on wireless communication systems. In 2012, he was assigned to ATR Wave Engineering Laboratories as a researcher and engaged in research and development on advanced techniques for frequency efficiency in satellite communication systems. His interest areas are wireless communication systems and digital signal processing. He is a regular member of the Institute of Electronics, Information and Communication Engineers (IEICE) of Japan.

Kazuto Yano received a B.E. degree in electrical and electronic engineering, M.S. and Ph.D. degrees in communications and computer engineering from Kyoto University in 2000, 2002, and 2005, respectively. He was a research fellow of the Japan Society for the Promotion Science (JSPS) from 2004 to 2006. In 2006, he joined the Advanced Telecommunications Research Institute International (ATR). Currently, he is a senior research scientist of the Wave Engineering Laboratories, ATR. His research interests include space-time signal processing for interference suppression, MIMO transmission, and PHY/MAC cross-layer design of cognitive radio for ISM bands. He received the IEEE VTS Japan 2001 Researcher's Encouragement Award, the IEICE Young Researcher's Award in 2007, the Ericsson Young Scientist Award 2007 and the IEICE 2007 Active Research Award in Radio Communication Systems. He also received 2010 Young Investigator Award in Software Radio from IEICE Technical Committee on Software Radio. He is a member of IEEE and IEICE.

Naoya Kukutsu received the B.E., M.E., and D.E. degrees in electrical engineering from Hokkaido University, Sapporo, Japan, in 1986, 1988 and 1991, respectively. His D.E. dissertation described research for a time-domain electromagnetic wave numerical analysis method. In 1991, he joined the Nippon Telegraph and Telephone Corporation (NTT), Applied Electronics Laboratories, and was engaged in developing high speed IC packages. From 2008-2013, he was a senior research engineer, supervisor at NTT Microsystem Integration Laboratories, and leader of the group that develops millimeter-wave and terahertz-wave radio transmission, as well as imaging systems. He is currently a senior research engineer at ATR Wave Engineering Laboratories and head of the department of Environment Communications. Dr. Kukutsu is a member of the IEEE MTT and COM Societies and a senior member of the Institute of Electronics, Information and Communication Engineers (IEICE).

Kiyoshi Kobayashi received the B.E., M.E. and Ph.D. degrees from Tokyo University of Science, Japan, in 1987, 1989 and 2004, respectively. He joined NTT Radio Communication Systems Laboratories in 1989. Since then, he has been engaged in the research and development of digital signal processing algorithms and their implementation techniques including modem, synchronization control and diversity for satellite and personal wireless communication systems. From 2011 to 2014, he was the director of ATR Wave Engineering Laboratories at Advanced Telecommunications Research Institute International, where he was engaged in research on advanced technologies for wireless communications. Currently, he is a senior research engineer, supervisor and a group leader of Satellite Communication Group in NTT Access Network Service Systems Laboratories, working on development of satellite communication systems. He is a member of IEEE and IEICE.

Tomoaki Kumagai received the B.E. and M.E. degrees in Electrical and Communication Engineering, and Ph.D. degree in Information Science from Tohoku University, Sendai, Japan, in 1990, 1992 and 2008, respectively. Since joining NTT in 1992, he has been engaged in research and development of personal communication systems and high-speed wireless LAN systems. Since 2014, he is the Director of Wave Engineering Laboratories, Advanced Telecommunications Research Institute International (ATR). He received the Young Engineer Award from the Institute of Electronics, Information and Communication Engineers (IEICE) in 1999. He is a member of the Institute of Electronics, Information and Communication Engineers (IEICE) and IEEE.